

Vortex-interface interactions and generation of glitches in pulsars

Armen Sedrakian and James M. Cordes

Center for Radiophysics and Space Research, Cornell University, Ithaca, NY 14853, USA

Accepted 1999 February 11. Received 1999 January 7; in original form 1997 December 8

ABSTRACT

We show that the crust-core interface in neutron stars acts as a potential barrier to the peripheral neutron vortices approaching the interface in the model in which these are coupled to the proton vortex clusters. This elementary barrier because of the interaction of vortex magnetic flux with the Meissner currents set up by the crustal magnetic field at the interface. The dominant part of the force is derived from the cluster-interface interaction. As a result of the stopping of the continuous neutron vortex current through the interface, angular momentum is stored in the superfluid layers in the vicinity of the crust-core interface during the interglitch period. Discontinuous annihilation of proton vortices on the boundary restores the neutron vortex current and spins up the observable crust on short time-scales, leading to a glitch in the spin characteristics of a pulsar.

Key words: MHD – stars: neutron – pulsars: general – stars: rotation.

1 INTRODUCTION

1.1 Motivation

The many-body calculations of the ground state energy of the matter in neutron stars imply an internal structure represented by succession of phase transitions as one moves from the surface to higher densities. The outer envelope of highly compressed solid melts into a homogeneous neutron-proton-electron Fermi liquid at roughly half the nuclear matter saturation density. The phase transition is an analog of the liquid-solid phase transition, is of the first order, and is signalled by an instability of the continuum proton liquid in the core against clustering into heavy nuclei in the crust (Pethick, Ravenhall & Lorenz 1995). In our subsequent discussion of the vortex-interface interaction we shall mainly focus on the crust-core interface and shall identify its location according to this criterion. The internal interface bounding the superfluid, superconducting neutron-proton liquid at supranuclear densities may correspond to either disappearance of the superfluidity of the nucleonic matter or onset of a kaon-condensed phase (e.g. Brown, et al 1994; and Pandharipande, Pethick & Thorsson 1995) or deconfined quark plasma (e.g. Glendenning 1996 and references therein). In view of the uncertainties involved in the physics of high-density nuclear matter, we shall only briefly discuss the vortex interactions with internal interfaces.

The density profiles of the superfluid phases in a neutron stars do not coincide with the profiles of various phases of dense matter in general. The boundaries of the latter phases thus may play an important role in the dynamics

of superfluids which support the vortex lattice state. For example, the rotation of neutrons is supported by a Feynman-Onsager vortex lattice state and their interaction with the phase boundaries can affect their dynamics; the same applies to the proton vortex lattices, carrying the magnetic flux through the superconducting proton liquid.

In the case of laboratory superfluids the vortex-interface interactions have been studied both experimentally and theoretically. An example is the onset of the resistive state in type-II superconductors when a current passes perpendicular to the applied magnetic field. The value of the critical current of sufficiently clean samples, where the pinning effects are negligible, remains finite, and is determined by the Bean-Livingstone barrier acting on the vortex lattice at the boundary. Experimental measurements on Nb by Lowell (1968) confirmed the existence of the barrier; a theoretical discussion can be found, for example, in de Gennes (1966). An example of manifestation of vortex-interface interaction in the neutral superfluids is the dependence of the lower critical velocity of vortex nucleation in superfluid ^4He on the roughness of the vessel inner surface (see e.g. Sonin & Krusius 1994).

In this paper we derive the vortex interface interactions occurring at the boundaries of the superfluid phases in neutron stars, and examine the conditions under which this type of interaction could be responsible for the phenomenon of glitches in the spins of pulsars. Any theoretical model should explain the following observational facts: (i) short spin-up time-scales, which are observed to be less than 120 s in the Vela pulsar B0833-45 and less than an hour

arXiv:astro-ph/9806042v2 26 May 1999

in the Crab pulsar B0531+21; (ii) magnitudes of the jumps in the rotation and spin-down rates, $\Delta\nu/\nu \sim 10^{-8} - 10^{-6}$ and $\Delta\dot{\nu}/\dot{\nu} \sim 10^{-3} - 10^{-2}$, respectively; and (iii) the origin of the instability driving a glitch, along with characteristic intervals between glitches for a given pulsar; the latter times-scales range from several months to several years depending on the object. The items (i)-(iii) will be addressed here using the vortex cluster model for the superfluid core dynamics (Sedrakian et al 1995a,b hereafter Papers I and II).

The physical picture is the following. In the interjump epoch a neutron star is decelerating; consequently the vortex lattice in the superfluid core is expanding and the peripheral vortices attempt to cross the crust-core boundary. The crust-superfluid core interface acts as a potential barrier to the proton vortices in the superfluid core that approach this boundary. If the repulsive component of the force, derived from the potential, is added to the force balance condition for the neutron vortices, it gives rise to an imbalance along the radial direction - the component of the friction force in this direction drops to zero, while the effective Magnus force becomes proportional to the difference between the velocities of the normal and superfluid components. The deceleration of the star will lead to a growth of this force until the proton vortices are able to annihilate at the interface. The neutron vortices will relax to their equilibrium positions, imparting angular momentum from the superfluid to the normal component thus, producing a pulsar macrojump. This picture is akin to the unpinning model of Anderson & Itoh (1975), except that the interaction does not involve the bulk of the superfluid, but rather its layer at the phase boundary. The latter setup has the advantage of a coherent onset of the glitch and does not require repinning. A brief sketch of this macrojump generation mechanism has been given elsewhere (Sedrakian & Cordes 1998).

1.2 Overview

The first suggested mechanisms for triggering the glitches were based on the idea of starquakes (Ruderman 1969; Smoluchowski & Welch 1970; Baym & Pines 1971; Carter & Quintana 1975). These models employed the idea of discontinuous readjustments of the shape of the star as it spins down under external dissipative torques. However, the possibilities of the explanation of the recurrence rate of glitches in the Vela and Crab pulsars within these models are severely limited; e.g. Baym & Pines (1971) find that the recurrence time is $\sim 10^8$ yr and $\sim 10^4$ yr for the Vela and Crab pulsars, respectively, if these are assumed to be $1.4 M_{\odot}$ neutron stars.

Instabilities associated with the superfluid component were proposed as being caused by long-living persistent currents and sudden annihilation of excess vortices (Packard 1972). A specific mechanism for the occurrence of the instability was proposed by Anderson & Itoh (1975), who argued that glitches occur through the pinning and unpinning of vortices in neutron star crusts [see also Anderson et al (1982) and Itoh (1983)]. The required moment of inertia that can be accumulated in the interglitch period and the mechanisms for the unpinning are suitable for the large glitches observed in Vela-type pulsars (Alpar et al 1981, 1993, Link & Epstein 1991). However the subsequent repinning, which

is required for the recurrence of glitches in this model, is still not well understood (Shaham 1980, Sedrakian 1995). Jones (1991a,1993) argued that the superfluid is not pinned in the whole bulk of the crusts, and the discontinuous relocation of the interface between the phases with pinned and unpinned vortices can trigger a glitch. Ruderman (1991) suggested that a spinning-down superfluid neutron star would strain the crust beyond its elastic yield strength, which would lead to crust cracking, resulting in glitches with magnitude and recurrence rate compatible with those observed. Thermal effects as a cause of a glitch were discussed by Greenstein (1979). Sudden perturbation of the inner crust temperature, leading to an increase of the frictional coupling between the superfluid and the crust, have been simulated by Link & Epstein (1996), who find spin-ups compatible with the glitches in the Crab and Vela pulsars. The effects of the exotic nuclear structure environment of the inner crust (e.g. Lorenz, Revenhall & Pethick 1993) on the vortex dynamics have been considered by Mochizuki, Oyamatsu & Izuyama (1997), who find that nuclear rod structure can pin a vortex line and can be an origin of vortex accumulation, leading to a glitch in the spirit of the Anderson-Itoh model.

Note that the glitch generation mechanisms, apart from describing the transients, lend themselves as candidates for generation of the sustained spin fluctuation processes manifested as ‘timing noise’ (Cordes & Greenstein 1981, Cordes, Downs & Krause-Polstorff 1988 and references therein). Simple amplitude down-scaling of the transients is not sufficient, however, because the transients are biased towards one sign of the spin-fluctuation (e.g. spin-up), while the timing noise fluctuations require deviations of both signs.

1.3 Organization of the paper

In Section 2 we derive general expressions for the vortex-interface interaction in three-velocity superfluid hydrodynamics and give order-of-magnitude estimates of the interaction strength at the crust-core interface. In Section 3 the collective interaction effects - the cluster-interface interaction - are discussed and a comparison with the Magnus force needed to build-up an instability is made. The microscopic time-scales relevant for the spin-up problem are considered in Section 4. Section 5 is a summary of our results.

2 VORTEX-INTERFACE INTERACTIONS IN THREE-VELOCITY HYDRODYNAMICS

We shall focus further on the dynamics of the superfluid outer core, where both the neutrons and the protons are in the superfluid state, and apply the Newtonian version of the superfluid hydrodynamics [a detailed exposition of the theory and references to earlier work can be found in Mendell & Lindblom (1991), Mendell (1991), and Paper I]. The relativistic counterparts of superfluid hydrodynamic equations have been made available recently (Langlouis, Sedrakian, Carter 1998, Carter & Langlouis 1998); their application to the problem at hand, however, is not straightforward and we shall continue to work entirely in the Newtonian limit.

To keep the discussion general, the ground state structure of vortex lattices will not be specified until Section 3. We will only assume that the protons form a continuum of

single particle states and that they are in the mixed type II superconducting state. As an outer interface bounding the neutron-proton superconducting phase we shall consider the crust-core interface, the location of which is identified with either the density of transition of the protons from a continuum to clustered state or the vanishing of neutron/proton superfluidity with decreasing density. For definiteness we shall proceed with the first condition, i.e. assume that the external interface is located at the position where the protons become unstable against clustering into nuclei. In that case the transition is first-order, and the interface is of the order of one nuclear spacing thick, in analogy with an ordinary liquid-solid interface (Pethick, Ravenhall & Lorenz 1995). The location of the inner core-outer core interface will be identified with the disappearance of the superconducting state of neutrons or protons with increasing density. For brevity we shall sometimes refer to these interfaces as the external and internal interfaces, respectively. The Bose condensation of mesons provides another possibility, that the inner interface is located at the density of the onset of the developed condensate.

2.1 Vortex - external interface interactions: cylindrical geometry

To set up the problem, assume that the crust supports a certain magnetic field of strength H_0 : a plausible origin for such a field could be the thermal battery effect (Blandford, Applegate & Hernquist 1983, Urpin, Levshakov & Yakovlev 1986) or the natal dynamo effect (Duncan & Thompson 1993). The type II superconducting protons in the core are assumed to be in the mixed state. The magnetic field, \mathbf{B}_v , of quantum vortices in the superfluid core is governed by the London equation for charged-neutral superfluid mixtures (Vardanian & Sedrakian 1981; Alpar, Langer & Sauls 1984; Sauls 1989):

$$\delta_p^2 \nabla \times (\nabla \times \mathbf{B}_v) + \mathbf{B}_v = \sum_{\tau} \nu_{\tau} \Phi_{\tau} \times \sum_q [\delta^{(2)}(\mathbf{r} - \mathbf{r}_{\tau q}^{(+)}) - \delta^{(2)}(\mathbf{r} - \mathbf{r}_{\tau q}^{(-)})], \quad (1)$$

where δ_p is the magnetic field penetration depth; the ν 's are circulation unit vectors; the q -summation is over the vortex sites in the two-dimensional vortex lattice plane; $\tau = \pm 1/2$ sums over the isospin projection; $\Phi_{1/2} \equiv \Phi_0$ is the flux quantum carried by proton vortices and $\Phi_{-1/2} \equiv k\Phi_0$ is the non-quantized flux of neutron vortices due to the entrainment effect; the entrainment coefficient k is a continuous function of nucleon effective masses (Andreev & Bashkin 1976; Vardanian & Sedrakian 1981; Alpar, Langer & Sauls 1984; Sauls 1989; the Fermi-liquid corrections to the entrainment coefficient have recently been discussed by Borumand, Joynt & Kluzniak 1996). The second term on the right-hand side of equation (1) takes into account the attractive part of the vortex-interface interaction in terms of vortex images of opposite sign, which are located symmetrically with respect to the crust-core interface. The total field at the crust-core interface, \mathbf{B} , is the superposition of the solution of equation (1),

$$\mathbf{B}_v = \sum_{\tau} \nu_{\tau} \frac{\Phi_{\tau}}{2\pi\delta_p^2}$$

$$\times \sum_q \left[K_0 \left(\frac{|\mathbf{r} - \mathbf{r}_{\tau q}^{(+)}|}{\delta_p} \right) - K_0 \left(\frac{|\mathbf{r} - \mathbf{r}_{\tau q}^{(-)}|}{\delta_p} \right) \right], \quad (2)$$

and the induction field \mathbf{B}_{cr} set up by the crustal field \mathbf{H}_0 , which exponentially penetrates in the superfluid core to a scale of the order of δ_p ; (here and below the K are the modified Bessel functions.) The magnetic field distribution with the proper boundary condition at the interface allows one to calculate the relevant part of the Gibbs free energy of the system $G = F - (4\pi)^{-1} \int \mathbf{B} \cdot \mathbf{H}_0 dV$, where the free-energy is

$$F = \frac{\delta_p^2}{8\pi} \int [\mathbf{B} \times (\nabla \times \mathbf{B})] \cdot d\mathbf{S} + \frac{\delta_p^2}{8\pi} \int \mathbf{B} \cdot [\delta_p^{-2} \mathbf{B} + \nabla \times (\nabla \times \mathbf{B})] dV. \quad (3)$$

The surface integration is over the crust-core interface, while the bulk integration involves the superfluid core region. Assume the vortex lattice plane is the (xy) -plane of Cartesian system of coordinates, with the interface being the (yz) -plane, and the circulation vectors in the superfluid core region are in the positive z -direction; the half-plane $x < 0$ corresponds to the crust while $x > 0$ corresponds to the superfluid core; see Fig. 1. The interactions, therefore, are x -dependent; the crustal magnetic field has a z -component of the form $B_{cr} = H_0 \exp(-x/\delta_p)$, and the boundary condition for the total magnetic field is $B_z = H_0$. Integrating equation (3), one finds $G = \sum_{\tau q} G_{\tau q}(x^{(+)})$, where

$$G_{\tau q}(x^{(+)}) = \frac{\Phi_{\tau}}{4\pi} \left\{ H_0 \exp\left(-\frac{x_{\tau q}^{(+)}}{\delta_p}\right) - H_0 + \frac{\Phi_{\tau}}{4\pi\delta_p^2} \left[\ln\left(\frac{\delta_p}{\xi}\right) - K_0\left(\frac{2x_{\tau q}^{(+)}}{\delta_p}\right) \right] + \sum_{\tau'} \frac{\Phi_{\tau'}}{4\pi\delta_p^2} \sum_{q'} \left[K_0\left(\frac{|x_{\tau' q'}^{(+)} - x_{\tau q}^{(+)}|}{\delta_p}\right) - K_0\left(\frac{|x_{\tau' q'}^{(+)} - x_{\tau q}^{(-)}|}{\delta_p}\right) \right] \right\}, \quad (4)$$

$x^{(+)}$ and $x^{(-)}$ denote the positions of the vortex and the image, respectively, and ξ is the coherence length of proton superconductor. Note that in the self-energy term we introduced a cut-off $K_0(x) \simeq \ln(\delta_p/\xi_p)$ for $x \rightarrow 0$. The primed summation assumes that the terms $q = q'$ and $\tau = \tau'$ are omitted.

The force associated with the interaction part of the Gibbs potential (4) is

$$f_{\tau q}(x^{(+)}) = \frac{\Phi_{\tau}}{4\pi} \left\{ \left[\frac{H_0}{\delta_p} \exp\left(-\frac{x_{\tau q}^{(+)}}{\delta_p}\right) - \frac{\Phi_{\tau}}{4\pi\delta_p^3} K_1\left(\frac{2x_{\tau q}^{(+)}}{\delta_p}\right) \right] + \sum_{\tau'} \frac{\Phi_{\tau'}}{4\pi\delta_p^3} \sum_{q'} \left[K_1\left(\frac{|x_{\tau' q'}^{(+)} - x_{\tau q}^{(+)}|}{\delta_p}\right) - K_1\left(\frac{|x_{\tau' q'}^{(+)} - x_{\tau q}^{(-)}|}{\delta_p}\right) \right] \right\}. \quad (5)$$

The first term in equation (5) corresponds to the repulsive force acting between the vortex magnetic flux and the

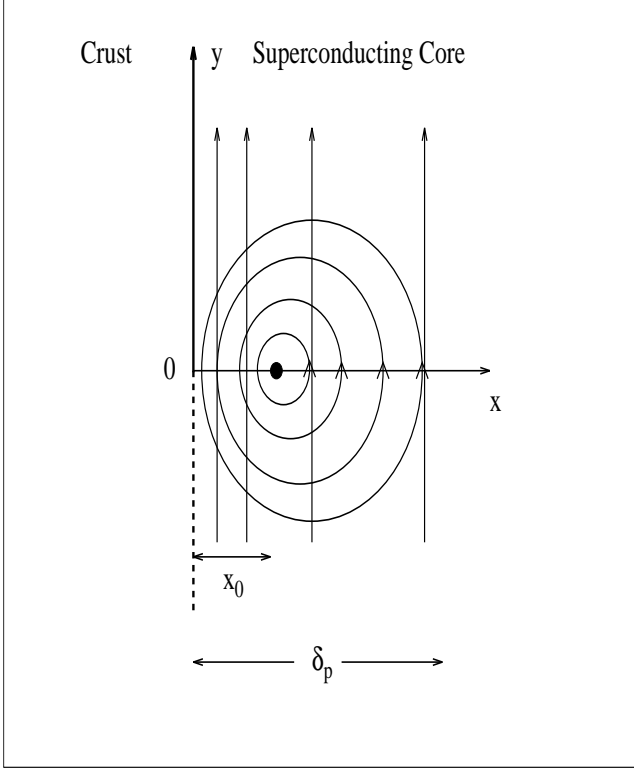


Figure 1. The geometry of vortex - crust-core interface interaction. The circles are the streamlines of the proton supercurrent circulation, which is screened beyond the scale δ_p . The Meissner currents (straight lines) induced by the crustal magnetic field penetrate within the superconducting core on the scale δ_p . The repulsive force arises because of the interference of oppositely directed Meissner currents and the vortex circulation. The attractive term arises because of the deformation of the vortex circulation near the boundary, where the density of the streamlines must be higher and, therefore, the superflow velocity is larger than on the opposite side of the vortex. This deformation is accounted for by adding the image of the vortex, as discussed in the text. The velocity gradients translate into pressure gradients, resulting in the vortex-interface interaction force.

crustal magnetic field. It can also be interpreted as a Lorentz force resulting from superposition of velocity fields of the vortex and the surface Meissner currents (Fig. 1). The second term is the force between the vortex and its image, which is attractive because of oppositely directed circulation vectors. The last two terms correspond to vortex-vortex and vortex-image interactions, respectively.

2.2 Single Vortex - Interface Interaction

To estimate the magnitude and asymptotics of the vortex-interface interaction, consider a single vortex with flux Φ_0 . From equation (5) we find

$$\bar{f}(\zeta) = [\bar{H} e^{-\zeta} - K_1(2\zeta)], \quad (6)$$

where the dimensionless variables are defined as $\bar{f}(\zeta) = f(x)/f^*$, $f^* = \Phi_0^2/8\pi^2\delta_p^3$, $\bar{H} = H_0/H^*$, $H^* = \Phi_0/2\pi\delta_p^2$, and $\zeta = x/\delta_p$. The function $\bar{f}(\zeta)$ is plotted in Fig. 2 for $\bar{H} = 0.003$. For large distances ($\zeta \rightarrow \infty$) the exponential

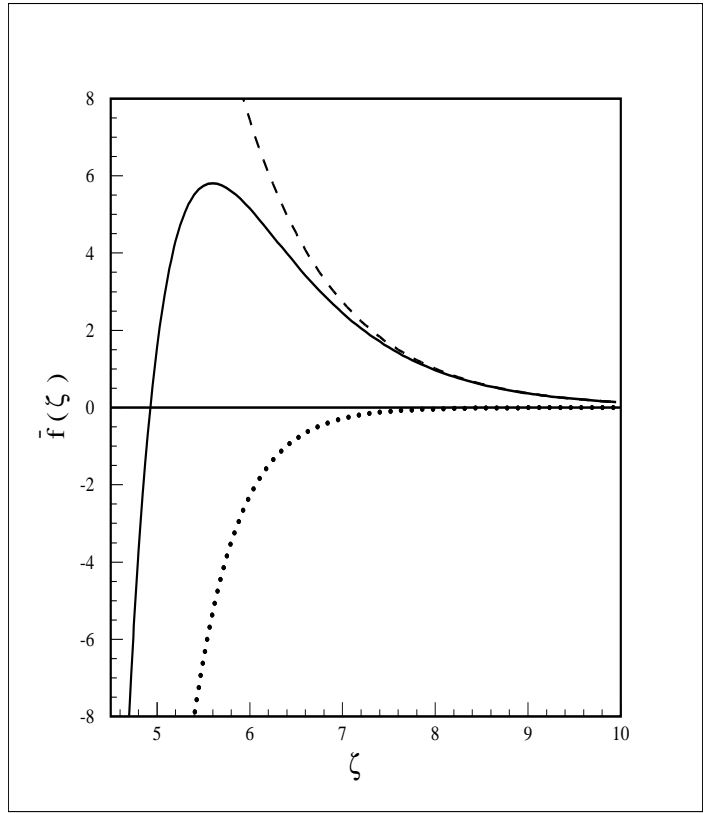


Figure 2. The dimensionless vortex-interface interaction force $\bar{f}(\zeta) \times 10^{-6}$ as a function of the reduced distance ζ for the crustal magnetic field value $H_0 = 10^{12}$ G (*full line*). The *dashed line* shows the repulsive component, while the *dotted line* is the attractive component of the force. For a discussion of the asymptotic behavior see the text.

(repulsive) term dominates, because in this limit the second term goes to zero more rapidly, [$K_1(2\zeta) \propto \sqrt{\pi/4\zeta} e^{-2\zeta}$]. For small distances the second (attractive) term in equation (5) dominates; note that it should be cut-off at $\zeta \sim \xi/\delta_p$ by replacing $K_1(2\xi/\delta_p)$ by $\delta_p/2\xi$. The repulsive part of the vortex - crust-core interface interaction, which dominates at large distances acts as a potential barrier to a vortex approaching the boundary, and thus prevents its continuous decay on the interface. If the magnitude of the crustal magnetic field is decreased, the potential barrier disappears in the limit $\bar{H} \rightarrow 0$.

The crust-core interface density will be identified with the density of separation of two phases where the protons are clustered in the nuclei (crust) and are in the continuum state (core). Following Pethick, Ravenhall & Lorenz (1995) we adopt the phase transition density $\rho_{tr} \simeq 1.56 \times 10^{14}$ g cm^{-3} . As pointed out earlier, the phase transition found in Pethick, Ravenhall & Lorenz (1995) is an analog of the ordinary first-order liquid-solid phase transition and the interface between the phases is one nuclear spacing thick. The stability of the interface requires a positive curvature energy associate with the interface between two phases; the system, therefore, will tend to minimize the surface of the interface. The typical scale of non-homogeneity should be the largest of the two relevant scales in the problem - the actual size of the

Table 1. Values of the maximal force for different applied magnetic fields.

$\log(H_0)$ [G]	$\overline{f}^{\max}(\zeta_0)$ [dyn/cm]	ζ_0
13	4.5×10^{-4}	3.6
12	5.8×10^{-6}	5.6
11	7.0×10^{-8}	7.6
10	7.8×10^{-10}	9.8
9	8.7×10^{-12}	12.1

nuclei and the size of the nuclear spacing. Both length scales are of the order of 30-50 fm. On the other hand, the interaction range, as can be seen from Fig. 2, is on order of 5-10 δ_p which translates into $1-5 \times 10^3$ fm for the value $\delta_p \simeq 200$ fm found at ρ_{tr} (see Table 2 later). As the interaction range exceeds the thickness of the interface by two orders of magnitude, the finite size of the interface can be ignored in the calculation of the force acting a vortex, which justifies the treatment above. Using the same transition density as above, we find $H^* \simeq 3.3 \times 10^{14}$ G, $f^* \simeq 5.4 \times 10^{17}$ dyn cm $^{-1}$ for $\delta_p = 100$ fm. Assuming a conventional value for the crustal magnetic field $H_0 = 10^{12}$ G, we obtain $H_0/H^* = 0.003$ and the maximum value of the reduced force $\overline{f}^{\max} \simeq 5.8 \times 10^{-6}$ at $\zeta = 5.6$. This translates to the maximal repulsive force $f^{\max} = f^* \overline{f}^{\max} \simeq 3.13 \times 10^{12}$ dyn cm $^{-1}$. In general, the magnitude of the crustal magnetic field at the crust-core interface for different objects can vary in a reasonable range, $10^9 < H_0 < 10^{13}$ G, though values beyond both extremes cannot be excluded. For further reference the values of the maximal force for different applied magnetic fields are given in Table 1. In the range of interest, the maximal force depends quadratically on magnitude of the crustal magnetic field.

2.3 Vortex - external interface interactions: spherical geometry

The vortex-interface interaction in its simplest form, equation (6), is easily generalized to the case where the vortex and the crustal magnetic field from an arbitrary angle with the spherical interface. Assume a straight vortex segment along the z direction of the cylindrical-polar coordinates. For a spherical interface of radius R we find:

$$\begin{aligned} \overline{f}(\varrho, \theta) &= \text{Sin } \theta \left[\overline{H}_z e^{-\zeta} - K_1(2\zeta) \right], \\ \zeta(\varrho, \theta) &= \delta_p^{-1} (R - \rho \text{Sin}^{-1} \theta), \end{aligned} \quad (7)$$

where ϱ is the distance of the vortex segment from the rotation axis in cylindrical coordinates with the origin at the z -axis, θ is the polar angle, \overline{H}_z is the projection of the crustal field on the z -axis. Because of the weak angle dependence of the force, our previous order of magnitude estimates remain valid unless the angle θ is close to zero, (i.e. the segment is close to the rotation axis). As the force vanishes exponentially for large arguments, it acts only at the ends of a vortex enclosed in a spherical shell. If the vortex is assumed to be straight, the averaging of the vortex - interface force over its length reduces the effective net force by the ratio of the effective range of the interaction to the length of the vortex. The vortices participating in the glitch generation process

need to adjust the (spherical) configuration of the interface in order to sustain the required magnitude of the Magnus force in the interjump period. In the spherical geometry this implies that the vortices, the ends of which are fixed at the interface, bend, forming an arc with a curvature radius of the order of R . The balance between the local tension force and the vortex-interface force determines whether the vortices in the bulk of the fluid will in fact bend under the action of the Magnus force. The magnitude of the force resulting from the vortex tension is given via the vortex self-energy as

$$f_T = \left(\frac{\Phi_0}{4\pi\delta_p} \right)^2 \ln \left(\frac{\delta_p}{\xi} \right) \mathcal{R}^{-1}, \quad (8)$$

where \mathcal{R} is the radius of the vortex curvature, with maximal value for the arc of the order of R . Assuming $\delta_p/\xi_p = 10$, $f_T = 5 \times 10^6$ dyn (R/cm) $^{-1}$, which is much smaller than the local vortex - interface interaction force. Thus, while the ends of the vortex are fixed at the interface, the Magnus force will bend the vortex in the bulk of the superfluid. Eventually the vortex will assume the form of the interface and the vortex-interface force will balance the Magnus force along the entire length of the vortex. Note that there is a cumulative increase of the vortex-interface force with the bending of the vortex - the larger the vortex curvature the larger is the net effective force. As the quantitative analysis now can be carried out using the local form of the force balance equation, in complete analogy to the previous discussion, we shall not repeat it here.

2.4 Vortex-internal interface interactions

The main difference between the physics of interaction of the vortices with the external and internal interfaces is that in the latter case the flux in the normal region enclosed in a superconductor must be quantized in units of Φ_0 (the superconducting region is multi-connected). For simplicity we shall consider a cylindrical geometry where external and internal interfaces are coaxial cylinders with the axis along the vector of rotation. The equilibrium value of the magnetic field in the inner normal core is established from a detailed balance between the processes of quantum flux capture from the superconducting region and flux drift in the superconducting region. In equilibrium, the number of quantum fluxes trapped in the internal region should minimize the energy of the system. The spin-down of the star or the Ohmic decay of the field within the normal core will drive the system out of equilibrium; e.g. if the magnetic field decreases in the inner core because of Ohmic dissipation, the flux transport into it would affect the dynamics of the neutron lattice requiring contractions, i.e. spin-ups in the angular velocity of the superfluid and, respectively, slow-downs in that of the crust. Conversely, spin-down would require formation of new vortices at the interface and their entrance into the superconducting region. The barrier at the inner core-outer core interface would prevent this processes from being continuous.

Let us derive the expression for the barrier at the inner interface. The magnetic field in the superconducting region bounded by two interfaces ($r_{\text{in}} \leq r \leq r_{\text{out}}$) is determined by the London equation (1) with the boundary conditions

$$B(r_1) = H_*, \quad B(r_2) = H_0, \quad (9)$$

where H_* is the magnetic field strength within the inner core. The solution of the homogeneous London equation is

$$B(r) = \frac{I_0(r)}{I_0(r_2)} H_0 [1 + \gamma(r)] - \gamma(r) \mathcal{H}, \quad (10)$$

where

$$\gamma(r) = \frac{K_0(r)I_0(r_2) - K_0(r_2)I_0(r)}{K_0(r_2)I_2(r_1) - K_2(r_1)I_0(r_2)} \quad (11)$$

and K_n and I_n are modified Bessel functions. Here the field \mathcal{H} is the sum of the quantized field trapped in the inner core and the field generated by the entrainment currents at the inner interface,

$$\mathcal{H} = \frac{q\Phi_0}{\pi r_1^2} + \frac{2mc|k|}{e}\Omega, \quad (12)$$

where q is an integer. The result (10) is derived by combining the equation for the circulation of the vector potential, \mathbf{A} , at the boundary of the inner core,

$$\oint \mathbf{A} \cdot d\mathbf{l} = \pi r_1^2 H_* \quad (13)$$

with the Maxwell equation for the magnetic field in the form

$$\delta_p^2 \left(\nabla \times \mathbf{B} - \frac{4\pi}{c} \mathbf{j}_{12} \right) = \frac{\Phi_0}{2\pi} \nabla \chi_1 - \mathbf{A}, \quad (14)$$

where χ_1 is the phase of the proton superconductor and $\mathbf{j}_{12} = \rho_{12} \mathbf{v}_2$ is the entrainment current (see Appendix ^{*}). For the geometry adopted (with cylindrical coordinates r, ϕ, z), the functions have simple azimuthal dependences; in particular the phase of proton supercurrent along the boundary is quantized:

$$(\nabla \chi)_\phi = \frac{q}{r}; \quad (15)$$

and

$$(\nabla \times \mathbf{B})_\phi = -\frac{\partial B_z}{\partial z}; \quad (\mathbf{j}_{12})_\phi = \frac{e}{m} \rho_{12} \Omega r, \quad (16)$$

where Ω is the rotation frequency and ρ_{12} is the density of the entrained protons. The total field is given by the sum of equation (11) and the particular solution equation (2) (owing to the short range of the spreading of the vortex field around the singularity, the vortex contribution to the boundary condition can be omitted). Knowledge of the total magnetic field allows one to calculate the Gibbs potential as before. One finds $G = \sum_{\tau q} G_{\tau q}(x^{(+)})$, where

$$\begin{aligned} G_{\tau q}(x^{(+)}) &= \frac{\Phi_\tau}{4\pi} \left\{ B \left(\frac{x_{\tau q}^{(+)}}{\delta_p} \right) - \mathcal{H} \right. \\ &+ \frac{\Phi_\tau}{4\pi \delta_p^2} \left[\ln \left(\frac{\delta_p}{\xi} \right) - K_0 \left(\frac{2x_{\tau q}^{(+)}}{\delta_p} \right) \right] \\ &+ \sum_{\tau'} \frac{\Phi_{\tau'}}{4\pi \delta_p^2} \sum_{q'} \left[K_0 \left(\frac{|x_{\tau' q'}^{(+)} - x_{\tau q}^{(+)}|}{\delta_p} \right) \right. \\ &\left. - K_0 \left(\frac{|x_{\tau' q'}^{(+)} - x_{\tau q}^{(-)}|}{\delta_p} \right) \right] \left. \right\}. \quad (17) \end{aligned}$$

^{*} Here and in the Appendix we use unconventional, but notationally convenient, isospin indices 1 and 2 for protons and neutrons respectively.

It can be seen that this result differs from that for the external interface in the functional form of the field at the interface. In deriving this result it has been assumed that the curvature of the inner surface is much larger than the size of a proton vortex and, therefore, the interface curvature can be ignored. The maximal force is given, as before, by the maximal value of the derivative of equation (17). The existence of the inner interface is a speculative issue because of our limited knowledge of the state of matter beyond several times the nuclear saturation density and the nature of pairing at these densities. We shall not evaluate quantitatively the results of this subsection. One may note, however, that if mesons form a Bose condensate, the interface between the proton superconductor and the pion/kaon condensate would have a barrier that would be a function of the differences in the magnetic field penetration depths of the condensates.

3 COLLECTIVE INTERACTIONS

3.1 Vortex Clusters

For further progress, we need to specify the ground state structure of vortices in the superfluid core. The proton vortices would mediate the interaction between the neutron vortices and the interface on quite general grounds because, first, the neutron and proton vortex interactions with the interface are of the same order of magnitude, and second, the total number of proton vortices per area of a neutron vortex is very large: $n_1 = (B/\Phi_0) (\kappa/2\Omega) = 2.5 \times 10^{13} B_{12} \Omega_{190}^{-1}$, where $\Phi_0 = \pi \hbar c/e$, $\kappa = \pi \hbar/m$ (m being the neutron mass) $B = 10^{12} B_{12}$ G is the mean magnetic field strength and $\Omega = 190 \Omega_{190} \text{ s}^{-1}$ is the spin frequency of the Crab pulsar.

We shall adopt here the vortex cluster model in which the distribution of 10^{13} proton vortex lines per neutron vortex is inhomogeneous and these are confined in a cluster around the neutron vortex (see Papers I and II). The scenario for vortex nucleation in the presence of the primordial magnetic field of a neutron star has been suggested by Baym, Pethick & Pines (1969); (see also Jones 1987 and references therein for the dynamics of uncoupled proton vortices in the core). They show that the Meissner state is preferable for fields lower than the lower critical field $H_{c1} \sim 10^{14}$ G; however, it cannot be achieved because the flux expulsion time is comparable to the lifetime of the pulsar. Therefore the field is forced to nucleate in the superconducting state via a *first-order* phase transition in a mixed state, even when this state is not the thermodynamically favoured one.

We suggest here a modified scenario which takes the advantage of the phase transition being of the first order. The kinetics of three-dimensional nucleation would initially require a field expulsion from randomly localized seeds of the superconducting state. The first-order phase transition would be realized via creation and subsequent expansion of the seeds of the stable (superconducting) phase within the metastable (normal) state. The nucleation process goes through two stages: first, formation of superconducting seeds of the critical size, which are, thus, stable against the collapse back into the normal state; and secondly, coalescence of supercritical seeds of the superconducting phase. This process would lead to a squeezing of the field into normal domains on microscales; when the size of the seeds of the superconducting phase becomes large enough, the field in the

normal domains will exceed H_{c1} . After this the nucleation of proton vortices will become energetically favorable. As the magnetic flux scales as the square of the linear size of a region, by flux conservation, the squeezing of an initially homogeneous field $\sim 10^{12}$ G over the area of a neutron vortex to a scale one order of magnitude smaller will drive the field intensity beyond the critical value $\sim 10^{14}$ G. The proton vortices will be arranged in clusters with linear size $\sim 0.1d_n$ (where d_n is the neutron inter-vortex spacing) and will sustain a mean magnetic field induction $\geq H_{c1}$. For fields higher than H_{c1} , the vortex state will nucleate in a homogeneous vortex structure.

Thermodynamic considerations show that intrinsic nucleation of clusters in response to the superfluid-dynamo is another possible mechanism; in this case, however, the structure and arrangement of the clusters can be predicted without resorting to kinetic theory of nucleation, and these are confined around the neutron vortex and are parallel to the neutron vortex lattice (see Papers I, II, and Appendix A of this paper).

What is the vortex cluster configuration when both creation mechanisms - those resulting from the residual field and the superfluid dynamo effect - are present? The answer perhaps depends on the sequence in which the neutron superfluidity and the proton superconductivity set in. The superfluid gap density profiles in the core show that the protons condense first; a naive expectation would be that the superfluid dynamo (present only if neutrons are superfluid) should operate in the presence of the proton vortex state because of the residual field. This might not be true because, on one hand, the first order transition to the superconducting state is commonly strongly delayed, so that the transition occurs from an overcooled state, and on the other hand, the pulsar temperature drops quickly below the critical temperatures of phase transitions. If both structures nucleate *independently*, their dynamics would be coupled via cluster-cluster interactions. An expression for the interaction force is given by the fourth line of eq. (5),

$$|\mathbf{f}_{\text{int}}| = \sum'_{\tau\tau'q'q} \boldsymbol{\nu}_\tau \cdot \boldsymbol{\nu}_{\tau'} \frac{\Phi_\tau \Phi_{\tau'}}{16\pi^2 \delta_p^3} \left[K_1 \left(\frac{|x_{\tau'q'}^{(+)} - x_{\tau q}^{(+)}|}{\delta_p} \right) \right], \quad (18)$$

except that in general it depends on the angle formed by the circulation vectors of the clusters $\boldsymbol{\nu}_\tau$. If this is less than a right angle the cluster would repel each other; in the opposite case these would merge and eventually annihilate. Note that the main contribution to this interaction comes from the changes in the *kinetic energy* of the clusters. A similar expression has been derived by Srinivasan et al. (1990), who recognize it as a repulsive force, Jones (1991b), Ruderman (1991), Mendell (1991) and Ding, Cheng & Chau (1993). The force is sometimes termed as a pinning interaction. Consistent with our treatment of the vortices as singular lines, the force does not include the modifications of the core energy of the vortex lines (Sauls 1989). Because of the large number of proton vortices collected in a cluster ($\sim 10^{13}$), the mutual creep considered by Ding, Cheng & Chau (1993) when the vortices form a homogeneous array, would be prohibited in our case by the large potential barrier of the vortex cluster.

While the problem of field nucleation and cluster-cluster interactions in the bulk of the superfluid needs more detailed

consideration, we shall restrict ourselves in the following material to clusters created by the superfluid dynamo effect. We believe that our results would not change qualitatively in a more elaborate picture.

3.2 Estimates

The localization radius of clusters, independent of the details of their nucleation mechanism, is of the order $\delta_n \sim 0.1 d_n$, where d_n is the neutron inter-vortex spacing (unless the initial field is larger than the lower critical one). As the proton intervortex distance $d_p \geq 10 \delta_p$ and the range of interaction is several times δ_p , a single row of vortices will interact with the interface. The number of vortices in a row is $N_\Phi \simeq \sqrt{8 \delta_n \delta_p / d_p^2}$.[†]

Using the value $d_p \geq 10^3$ fm for a Vela-type pulsar, one finds $N_\Phi \simeq 283$. The maximal force on the vortex cluster, therefore, is $f_C^{\text{max}} = N_\Phi f^{\text{max}} = 8.9 \times 10^{14}$ dyn cm⁻¹. The repulsive component of the vortex-interface interaction force would require an increase in the Magnus force by a magnitude

$$f^M = 3.23 \times 10^{17} \left(\frac{\delta\omega_s}{\text{s}^{-1}} \right) \times \left(\frac{\nu}{1.98 \times 10^{-3} \text{ cm}^2 \text{ s}^{-1}} \right) \left(\frac{R}{9.6 \times 10^5 \text{ cm}} \right) \quad (19)$$

per neutron vortex, in order to restore the free-flow expansion of the neutron vortex lattice through the interface. Here ρ_s is the superfluid density, $\nu = \pi\hbar/m_n$, m_n is the neutron mass, R is the distance of the crust-core boundary from the rotation axis, and $\delta\omega_s$ the angular velocity departure between the superfluid and the normal components.[‡] From the balance condition $f_C^{\text{max}} = f^M$ one finds the value of the maximal departure $\delta\omega_s^{\text{max}} \simeq 0.003$ s⁻¹ that can be sustained by the boundary force on the cluster. Note that although the vortex-interface force is effectively acting on the outermost neutron vortex dressed by a proton vortex cluster, the long-range neutron vortex-vortex interaction ensures that the force is acting on a macroscopic domain of neutron vortex lattice.

One can now estimate whether the effective magnitude of the moment of inertia of the superfluid vortex domain near the crust-core interface, which has short (≤ 120 s) dynamical coupling times, is sufficient to drive a large Vela-type glitch, provided the angular velocity departure has reached its critical value $\delta\omega_s^{\text{max}}$. Note that, although the range of the interaction is microscopic, a macroscopic region of the superfluid neutron vortex lattice will undergo compression because of stopping of the continuous vortex current through the interface. For large Vela glitches, the magnitude of the jump in the rotation rate of the normal component is $\delta\omega/\omega \sim 10^{-6}$. Using the angular momentum

[†] This estimate follows from the observation that the length of a row lying within the range of the interaction from cluster's circular boundary is $2\sqrt{\delta_n^2 - (\delta_n - \Lambda)^2} = 2\sqrt{2\delta_n\Lambda + O(\Lambda^2)}$, where δ_n is the cluster radius, $\Lambda \sim \delta_p$ is the effective range of the interaction. The number of vortices is obtained by dividing the length of the row by the lattice constant $\sim d_p$.

[‡] The neutron star model used in our estimates is discussed in detail in Paper II.

conservation $I_s \delta \omega_s^{\max} = I_n \delta \omega$, where I_s and I_n are the moment of inertia of the superfluid and normal components, respectively, for the Vela pulsar we find $I_s/I_n = 0.023$. For a comparison with the model calculations one needs to know the moment of inertia of the normal component which undergoes the observed spin-up. For the neutron star model described in Paper I, we find $I_s/I_n = 0.017$ assuming that the I_n is the whole crust. This number is close to the estimate above, but is uncertain because of our limited knowledge of the number of components of the star involved in the short spin-up process.

4 SPIN-UP TIMESCALES

In discussing the spin-up time-scales we shall assume that the spin-up of the normal component (or at least the layers relevant for generation of the glitch) can be separated from the spin-up of the superfluid due to the mutual friction. Our conclusions can be modified in a combined treatment of the normal and superfluid components, because the spin-up times for the core plasma (in the Vela pulsar) are of the same order of magnitude as that for the superfluid. Easson (1979) has discussed the Ekman pumping mechanism of the normal component and has found spin-up time-scales on the order of 10 s. Stratification effects (Goldreich & Reisenegger 1992) change this picture; in particular the Ekman pumping cannot explain the fast core-crust coupling in the Vela pulsar (Abney, Epstein & Olinto 1996). Lee (1995) and Mendell (1998) discussed the coupling via the superfluid oscillations; the cyclotron-vortex waves were identified as a being important ingredients of the spin-up process (Mendell 1998).

Let us first consider the dynamics of the electron liquid and separate the volume per single neutron vortex in the region including the proton vortex cluster $V_<$ and the remaining volume, $V_>$, which is free of magnetic flux. The collision integral in the Landau-Boltzmann equation for the electron distribution receives its two main contributions from electron-electron (e - e) and electron-proton vortex (e - Φ) collisions. The rate of the first process is given by the reciprocal of the lifetime of a quasiparticle in a relativistic electron Fermi-liquid, τ_{ee} , as

$$\tau_{ee}^{-1} = \frac{\pi^3}{16} \frac{(k_B T)^2}{\hbar \epsilon_{eF}} F(\beta), \quad (20)$$

where T is the temperature, k_B is the Boltzmann constant, $\epsilon_{eF} = \hbar c k_{Fe}$ is the Fermi energy of electrons, k_{Fe} is the electron Fermi wave number, and

$$F(\beta) = \frac{\beta}{1+\beta} + \beta^{1/2} \sin^{-1}(1+\beta)^{-1/2} - \frac{\beta}{(1+2\beta)^{1/2}} \cos^{-1} \left(\frac{\beta}{1+\beta} \right) \quad (21)$$

is a correction arising due to the finite range of the interaction, where $\beta = k_{TF}^2 / 4k_{Fe}^2$ and k_{TF} is the Thomas-Fermi screening length of protons (Smith & Hojgaard Jensen 1989; for the screening effects see Baym et al 1969). The rate for the second process, electron-flux scattering, in the volume $V_<$ is

$$\tau_{<}^{-1} = \frac{3\pi^3}{64} \frac{c \delta_p}{(k_e \delta_p)^2} \frac{\bar{B}}{\Phi_0}, \quad (22)$$

where $\bar{B} \simeq 10^{14}$ G is the mean magnetic field of the cluster. In the volume $V_>$ the e - e rates are given by the same expression (20), however the electron flux scattering is only on the boundaries of the clusters. The rate of this process can be estimated as

$$\tau_{>}^{-1} \simeq n_n c d_n \left(\frac{\xi_p}{\delta_p} \right)^{1/2|k|}, \quad (23)$$

where n_n is the neutron vortex number density, which is related to the neutron vortex (triangular) lattice constant, d_n , by the relation $n_n = 2/\sqrt{3} d_n^2$. This estimate does not take into account the finite ‘skin’ of the cluster and a more precise calculation would require inclusion of the structure factor of the vortex cluster, which would lead to somewhat larger scattering rates. The estimate (23), which assumes an impenetrable cluster, is the opposite limit of the relaxation time found in Paper I, which assumes a transparent cluster. These time-scales give the upper and lower bounds on the relaxation times, although the first one should be closer to the exact value. The ratio of these time-scales is of order of unity in the density region of interest, but can increase by two orders of magnitude at high densities. The values of relaxation times along with the relevant microscopic parameters (Baldo et al 1992) are given in Table 2.

The last two columns give the corresponding viscosity and the dynamical spin-up time scale. It can be seen that in the region $V_<$ one has $\tau_{ee} \gg \tau_<$, which means that electrons are localized within the clusters (i.e. the electrons equilibrate among themselves much slower than with the vortex lattice). In this case the electron fluid can not be ascribed an independent velocity and its transport is controlled by the dynamics of the cluster. In the main region $V_>$ (note that $V_>/(V_< + V_>) \sim 90\%$) the opposite limit $\tau_{ee} \ll \tau_>$ is realized and therefore the electron fluid is an independent entity and couples to the clusters by viscous friction. This situation is illustrated in Fig. 3.

The value of the viscous friction (or mutual friction) coefficient is related to $\tau_>$ as $\eta = (n_e/n_n)(\epsilon_{eF}/c^2 \tau_>)$, where n_e is the electron density. The values of the spin-up time (Table 2), which are identified with the dynamical coupling times of the superfluid shell at the crust-core interface (Paper II), are compatible with the requirement placed by the Christmas glitch observation of the Vela pulsar.

5 CONCLUSIONS

The main features of the present model and the predictions that can be drawn from these are as follows:

(i) The glitch activity depends on the geometry of the crustal and core magnetic fields. If the generated field is anti-parallel to the spin axis (as predicted by the generation scenario) the inclination of the crustal field larger than 90° would be necessary in order to produce a repulsive barrier to peripheral neutron vortices. If the crustal field geometries are restricted, then correlations between the glitch activity and the surface magnetic field values derived from (e.g.) the magnetic dipole radiation formula are expected. If this is not the case, pulsars with similar characteristics (e.g. age) might show very different glitch activity.

Table 2. Value of relaxation times and various microscopic parameters.

ρ $\times 10^{14}$ g cm $^{-3}$	k_{Fe} fm $^{-1}$	$ k $	δ_p fm	ξ fm	τ_{ee} $\times 10^{-15}$ s	$\tau_{<}$ $\times 10^{-17}$ s	$\tau_{>}$ s	η g cm $^{-1}$ s $^{-1}$	τ_d min
1.67	0.41	0.14	161.17	6.57	1.58	3.85	2.60e-09	1.62e+15	6.23e-01
1.84	0.40	0.18	149.69	7.01	1.57	3.48	4.84e-10	8.25e+15	2.90+00
2.00	0.46	0.20	140.05	7.51	1.88	4.14	1.43e-10	4.50e+16	1.45e+01
2.50	0.52	0.25	118.08	9.09	2.32	4.50	1.75e-11	6.11e+17	1.58e+02

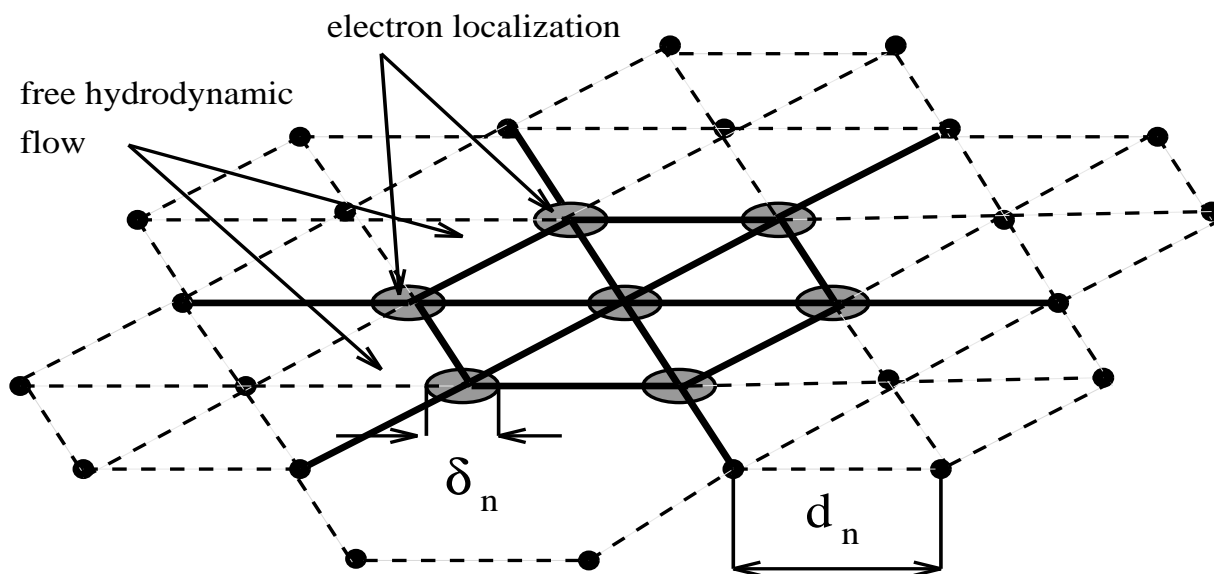


Figure 3. This figure shows the triangular neutron vortex lattice with the lattice constant d_n . The shaded regions display the clusters of effective size δ_n . The electrons form a hydrodynamic fluid in the intervening space between the cluster and are localized within the vortex clusters, providing a charge neutralizing background.

This type of observation could support our model, because this type of behaviour cannot be understood within known models of glitch generation.

(ii) For millisecond pulsars with low magnetic fields ($\sim 10^9$ G) the vortex-interface interaction force would be 6 orders of magnitude lower than for conventional pulsars ($H_0 \sim 10^{12}$ G), implying interjump periods comparable to the evolutionary time-scales and, therefore, a marginal glitch activity.

(iii) The occurrence of the glitch would require small changes in the geometry of the compound field of the pulsar and possibly changes in the inclination angle of the dipole field. The location of the barrier at a fixed interface (with the same physical parameters for the whole system) and the homogeneity of the environment of the superfluid phase suggests consistency in the conditions at the onset of instability driving the glitch, which appears to be one of the advantages of the present model.

(iv) The thermal effects do not appear as an input; the release of the self-energy of the vortex lines at the crust-core boundary might, however, provide a considerable heat flux (and the stationary situation is discussed in Sedrakian & Sedrakian 1993). Thermal pulse observation associated with a glitch (Eichler & Cheng 1989, Van Riper, Epstein & Miller 1991, Chong & Cheng 1994, Hirano et al 1997) can be caused by the vortex annihilation at the crust core boundary. This type of heating may serve as an input for the thermally activated glitches (Link & Epstein 1996).

(v) The model does not invoke any type of quake activity, but may trigger magnetic field configuration changes, which may induce plate tectonic activity (Ruderman 1991). The opposite may be true, i.e. the plate tectonic activity (Ruderman 1991) could allow the proton vortices to overcome the barrier and trigger a runaway instability at the the crust core interface.

To summarize, a potential barrier, resulting from magnetic interaction between the proton vortices and the crustal magnetic field at the crust-core interface, is suggested as the possible mechanism for the generation of pulsar glitches. It is shown that the force derived from that potential can sustain a Magnus force in an interjump period within a superfluid region with sufficient moment of inertia and appropriate dynamical coupling times in order to generate a large glitch, like those observed in the Vela-type pulsars.

ACKNOWLEDGMENTS

This work was supported by NSF Grant 9528394 to Cornell University. AS gratefully acknowledges a research grant from the Max Kade Foundation, New York.

REFERENCES

Abney, M., Epstein, R., Olinto, A. V., 1996, *ApJ*, 466, L91
 Alpar, M. A., Anderson, P. W., Pines, D., Shaham, J., 1981, *ApJ*, 249, L33
 Alpar, M. A., Chau, H. F., Cheng, K. S., Pines, D., 1993, *ApJ*, 409, 345
 Alpar, M. A., Langer, S. J., Sauls, J. A., 1984, *ApJ*, 282, 533
 Anderson, P. W., Itoh, N., 1975, *Nature*, 256, 25

Anderson, P.W., Alpar, M.A., Pines, D., Shaham, J., 1982, *Phil. Mag. A*, 45, 227
 Andreev, A. F., Bashkin, E. P., 1976, *Sov. Phys. - JETP*, 42, 164
 Baldo M., Cugnon J., Lejeune A., Lombardo U., 1992, *Nucl. Phys. A*, 536, 349
 Baym, G., Pines, D., 1971, *Ann. Phys.*, 66, 816
 Baym, G., Pethick, C., Pines, D., 1969, *Nature*, 224, 673
 Blandford, R. D., Applegate, J. H., Hernquist, L., 1983, *MNRAS*, 204, 1025
 Borumand, M., Joynt, R., Kluzniak, W., 1996, *Phys. Rev. C*, 54, 2745
 Brown, G., Lee, C., Rho, M., Thorsson, V., 1994, *Nucl. Phys A*, 572, 693
 Carter, B., Quintana, H., 1975, *ApJ*, 202, 511
 Carter, B., Langlois, D., 1998, *Nucl. Phys. B*531, 478
 Chong, N., Cheng, K. S., 1994, *ApJ*, 425, 210
 Cordes J. M., Greenstein G., 1981, *ApJ*, 245, 1060
 Cordes, J. M., Downs G., Krause-Polstorff, J., 1988, *ApJ*, 330, 847
 Duncan, R. C., Thompson, C., 1993, *ApJ*, 408, 194
 de Gennes, P.-G., 1966, *Superconductivity of metals and alloys*, Benjamin, New York
 Ding, K. Y., Cheng, K. S., Chau, H. F., 1993, *ApJ*, 408, 167
 Easson, I., 1979, *ApJ*, 228, 257
 Eichler, D., Cheng, A. F., 1989, *ApJ*, 336, 360
 Glendenning, N. K., 1996, *Compact Stars*, Springer, New York
 Goldreich, P., Reisenegger, A., 1992, *ApJ*, 395, 250
 Greenstein, G., 1979, *ApJ*, 321, 521
 Shaham, J., 1980, *J. de Phys.*, 41, C2-9
 Hirano, S., Shibazaki, N., Umeda, H., Nomoto, K., 1997, *ApJ*, 491, 286
 Itoh, N., 1983, *Prog. of Theor. Phys.*, 69, 338
 Jones, P. B., 1987, *MNRAS*, 228, 419
 Jones, P. B., 1991a, *ApJ*, 373, 208
 Jones, P. B., 1991b, *MNRAS*, 253, 279
 Jones, P. B., 1993, *MNRAS*, 263, 619
 Langlois, D., Sedrakian, D. M., Carter B., 1998, *MNRAS*, 297, 1189
 Lee, U., 1995, *A&A*, 303, 515
 Link, B., Epstein, R. I., 1991, *ApJ*, 373, 592
 Link, B., Epstein, R. I., 1996, *ApJ*, 457, 844
 Lorenz, C. P., Ravenhall, D. G., Pethick, C. J., 1993, *Phys. Rev. Lett.*, 70, 379
 Lowell, J., 1968, *Phys. Lett. A*, 26, 111
 Mendell, G., Lindblom, L., 1991, *Ann. Phys.*, 205, 110
 Mendell, G., 1991, *ApJ*, 380, 515
 Mendell, G., 1998, *MNRAS*, 296, 903
 Mochizuki, Y., Oyamatsu, K., & Izuyama, T., 1997, *ApJ*, 489, 848
 Packard, R. E., 1972, *Phys. Rev. Lett.*, 28, 1080
 Pandharipande, V. R., Pethick, C. J., Thorsson, V., 1995, *Phys. Rev. Lett.*, 75, 4567.
 Pethick, C. J., Ravenhall, D. G., Lorenz, C. P., 1995, *Nucl. Phys. A*, 584, 675
 Ruderman, M., 1969, *Nature*, 223, 597
 Ruderman, M., 1991, *ApJ*, 382, 587
 Sauls, J. A., 1989, in ed. Ogelman H., van den Heuvel E. P. J., eds, *Timing Neutron Stars*, Kluwer, Dordrecht, p. 479
 Sedrakian A., Cordes J., 1998, in: Olinto A., Frieman J., Schramm D., eds, *Relativistic Astrophysics and Cosmology*, World Scientific, Singapore. (astro-ph/9709277)
 Sedrakian, A. D., 1995, *MNRAS*, 277, 225
 Sedrakian, A. D., Sedrakian, D. M., 1993, *ApJ*, 413, 6588
 Sedrakian, A. D., Sedrakian, D. M., 1995a, *ApJ*, 447, 305 (Paper I)
 Sedrakian, A. D., Sedrakian, D. M., Cordes, J. M., Terzian, Y., 1995b, *ApJ*, 447, 324 (Paper II)

- Sedrakian, D. M., Shakhbasian, K. M., Movssisian A. G., 1983, *Astrophysics*, 19, 175
- Smith, H., Hojgaard Jensen, H., 1989, *Transport Phenomena*, Clarendon, Oxford, pg. 199.
- Sonin, E. & Krusius, M. 1994, in: *The Vortex State*, eds. Bon-tempis et al., Kluwer, Boston.
- Smoluchowski, R., Welch, D., 1970, *Phys. Rev. Lett.*, 24, 1191
- Srinivasan, G., Bhattacharya, G., Muslimov, A., Tsygan, S. 1990, *Current Sci*, 59, 31
- Urpin, V. A., Levshakov, S. A., Yakovlev, D. G., 1986, *MNRAS*, 219, 703
- Van Riper, K. A., Epstein, R. I., Miller, G. S., 1991, *ApJ*, 381, L47
- Vardanian, G. A., Sedrakian, D. M., 1981, *Sov-Phys. JETP*, 54, 919

APPENDIX A: GROUND STATE VORTEX CONFIGURATIONS

In this appendix we recapitulate several results regarding magnetic structure of the neutron vortex lattice. These has been previously obtained by Vardanian & Sedrakian (1981) and Sedrakian et al (1983) in a hydrodynamic approach and by Alpar, Langer & Sauls (1984) using an effective Ginzburg-Landau theory. Here we employ a variational minimization method, which allows us to illuminate several aspects of the problem which have not been exposed previously.

Consider a rotating Fermi-liquid mixture of superfluid neutrons, superconducting protons and normal electrons. At temperatures of interest the number of quasiparticle excitations is negligible. The electron system executes a rigid body rotation with angular velocity $\boldsymbol{\Omega}$. The kinetic energy of the neutron superfluid, which is by far the dominant part of the energy of the system, is minimized by a lattice of neutron vortices. This allows for a coarse-grained rigid body rotation of the superfluid with the angular velocity $\boldsymbol{\Omega}$. If the interaction between neutrons and protons is switched on, the entrainment effect does not changes this result to any considerable extent: the correction to the mass current of the neutrons is of the order of the ratio of proton to neutron density, while the resulting magnetic energy density of the system is by orders of magnitude lower than the kinetic energy density. Below we shall assume that the neutron superflow pattern is determined by the minimization of the kinetic energy of this system and consider the behaviour of the proton superconductor.

The gradient invariant superfluid velocities are defined as [§]

$$\mathbf{v}_1 = \frac{\hbar}{2m_1} \nabla \chi_1 - \frac{e}{m_1 c} \mathbf{A}, \quad (\text{A1})$$

$$\mathbf{v}_2 = \frac{\hbar}{2m_2} \nabla \chi_2, \quad (\text{A2})$$

where m denotes the mass, χ the phase of the superfluid order parameter and \mathbf{A} the vector potential; the isospin indices 1 and 2 refer to protons and neutrons respectively. Taking the curl of equations (A1) and (A2) and accounting for the

[§] Note that in the rotating frame all velocities acquire a constant $\boldsymbol{\Omega} \times \mathbf{r}$ term, which however does not affect the result of variational calculation and therefore will be omitted everywhere below.

quantization of the phase of superfluid order parameter, one finds

$$\text{curl } \mathbf{v}_1 = \nu_1 \frac{\pi \hbar}{m_1} n_1 - \frac{e}{m_1 c} \mathbf{B}, \quad (\text{A3})$$

$$\text{curl } \mathbf{v}_2 = \nu_2 \frac{\pi \hbar}{m_2} n_2 \quad (\text{A4})$$

where n stands for the number density of vortices, $\boldsymbol{\nu} = (\text{curl } \mathbf{v}) / |\text{curl } \mathbf{v}|$ and $\mathbf{B} = \text{curl } \mathbf{A}$. The Maxwell equation for the magnetic field is

$$\text{curl } \mathbf{B} = \frac{4\pi e}{m_1 c} (\rho_{11} \mathbf{v}_1 + \rho_{12} \mathbf{v}_2), \quad (\text{A5})$$

where ρ_{11} and ρ_{12} are unentrained and entrained parts of the proton condensate density. We define auxiliary functions \mathbf{B}_1 and \mathbf{B}_2 by the following relations:

$$\text{curl } \mathbf{B}_1 \equiv \frac{4\pi e}{m_1 c} \rho_{11} \mathbf{v}_1, \quad (\text{A6})$$

$$\text{curl } \mathbf{B}_2 \equiv \frac{4\pi e}{m_2 c} \rho_{12} \mathbf{v}_2. \quad (\text{A7})$$

According to eq. (A5) $\mathbf{B} = \mathbf{B}_1 + \mathbf{B}_2$. Taking the curl of equations (A6) and (A7) and using equations (A3) and (A4) one finds

$$\begin{aligned} \text{curl curl } \mathbf{B}_1 &= \frac{4\pi e}{m_1 c} \rho_{11} \left(\nu_1 \frac{\pi \hbar}{m_1} n_1 - \frac{e}{m_1 c} \mathbf{B} \right) \\ &= \delta_p^{-2} (\nu_1 \Phi_0 n_1 - \mathbf{B}), \end{aligned} \quad (\text{A8})$$

$$\text{curl curl } \mathbf{B}_2 = \nu_2 \frac{4\pi e}{m_2 c} \rho_{12} \frac{\pi \hbar}{m_2} n_2 = \nu_2 \delta_p^{-2} \Phi_1 n_2, \quad (\text{A9})$$

where

$$\delta_p^2 = \frac{m_1^2 c^2}{4\pi e^2 \rho_{11}}, \quad \Phi_0 = \frac{\pi \hbar c}{e}, \quad \Phi_1 = \frac{\rho_{12}}{\rho_{11}} \Phi_0. \quad (\text{A10})$$

The free-energy of the superfluid neutron-proton mixture reads

$$\mathcal{F} = \frac{1}{2} \int (\rho_{11} v_1^2 + 2\rho_{12} \mathbf{v}_1 \cdot \mathbf{v}_2 + \rho_{22} v_2^2) dV + \int \frac{B^2}{8\pi} dV \quad (\text{A11})$$

The free energy is a functional of the neutron and proton superfluid velocities. Once the minimization with respect of the neutron superfluid velocity is performed, the proton superflow pattern is determined by the minimum of this functional with respect to \mathbf{v}_1 at constant \mathbf{v}_2 . The respective variation of the functional (A11) is

$$\begin{aligned} \delta \mathcal{F} &= \int (\rho_{11} \mathbf{v}_1 + \rho_{12} \mathbf{v}_2) \cdot \delta \mathbf{v}_1 dV \\ &+ \frac{1}{4\pi} \int (\mathbf{B}_1 + \mathbf{B}_2) \cdot \delta \mathbf{B}_1 dV. \end{aligned} \quad (\text{A12})$$

Alternatively, using equation (A6) to eliminate \mathbf{v}_1 in favor of \mathbf{B}_1 , one finds

$$\begin{aligned} \delta \mathcal{F} &= \frac{\delta_p^2}{4\pi} \int (\text{curl } \mathbf{B}_1 + \text{curl } \mathbf{B}_2) \cdot \text{curl } \delta \mathbf{B}_1 \\ &+ \frac{1}{4\pi} \int (\mathbf{B}_1 + \mathbf{B}_2) \cdot \delta \mathbf{B}_1 dV \\ &= \frac{1}{4\pi} \int [\mathbf{B}_1 + \mathbf{B}_2 + \delta_p^2 \text{curl curl } (\mathbf{B}_1 + \mathbf{B}_2)] \cdot \delta \mathbf{B}_1 dV. \end{aligned} \quad (\text{A13})$$

Here, to obtain the third line, we used the relation $\text{curl } \mathbf{a} \cdot \mathbf{b} - \mathbf{b} \cdot \text{curl } \mathbf{a} = \text{div}[\mathbf{b} \times \mathbf{a}]$ and the assumption that surface integral

over the boundary of the system vanishes (note that this is not true at the crust-core interface!) As $\delta\mathbf{B}_1$ is arbitrary, the minimum (more precisely extremum) condition implies that the expression in the bracket must vanish identically. Using equations (A8) and (A9) this condition takes the simple form

$$\Phi_1 n_2 + (\boldsymbol{\nu}_1 \cdot \boldsymbol{\nu}_2) \Phi_0 n_1 = 0 \quad (\text{A14})$$

or, apart from the situation when $\boldsymbol{\nu}_1 \cdot \boldsymbol{\nu}_2 = 0$,

$$n_1 = \frac{|k|}{\boldsymbol{\nu}_1 \cdot \boldsymbol{\nu}_2} n_2. \quad (\text{A15})$$

(Note that the entrainment coefficient is negative). This result shows that the actual flux of the neutron vortex is $\Phi_1 \pm q\Phi_0$, where q is an integer different from zero, which is in contrast to previous general knowledge.

The derivation above has a definite subtlety, because we ignored the fact that for the superconducting proton subsystem not only is the velocity field \mathbf{v}_2 fixed, but according to (A7) the field component \mathbf{B}_2 is fixed as well. This fact can be visualized by taking the limit of perfect entrainment ($|k| \rightarrow 1$). In this idealized case the whole proton superconductor follows the neutron vortex circulations and the corresponding magnetic field is unscreened (its logarithmic divergence is cut-off by the finite size of the system).

If the entrainment is imperfect, then part of the superconducting proton condensate is available either for Meissner screening the field or squeezing it into flux tubes. The presence of the background field \mathbf{B}_2 implies that one should seek the minimum of the Gibbs thermodynamical potential ($\mathcal{F} - \mathbf{B} \cdot \mathbf{B}_2/4\pi$):

$$\begin{aligned} \mathcal{G} &= \frac{1}{2} \int (\rho_{11} v_1^2 + 2\rho_{12} \mathbf{v}_1 \cdot \mathbf{v}_2 + \rho_{22} v_2^2) dV \\ &+ \int \frac{B^2}{8\pi} dV - \int \frac{\mathbf{B} \cdot \mathbf{B}_2}{4\pi} dV. \end{aligned} \quad (\text{A16})$$

The variation of the Gibbs free-energy (which goes in a full analogy with the foregoing discussion for $\delta\mathcal{F}$) leads to the condition

$$(\Phi_1 n_2 - B_2) + (\boldsymbol{\nu}_1 \cdot \boldsymbol{\nu}_2) \Phi_0 n_1 = 0, \quad (\text{A17})$$

or

$$(\boldsymbol{\nu}_1 \cdot \boldsymbol{\nu}_2) n_1 = \frac{(B_2 - n_2 \Phi_1)}{\Phi_0}. \quad (\text{A18})$$

For a region far from the neutron vortex one finds

$$n_1 = \frac{B_2}{\Phi_0}, \quad (\text{A19})$$

where we used the fact that the configuration $(\boldsymbol{\nu}_1 \cdot \boldsymbol{\nu}_2) = 1$ would require the smallest value of n_1 . The value of B_2 is determined by integration of eq. (A7) for a given neutron superflow \mathbf{v}_2 . In particular, for a single neutron vortex this would be the familiar superfluid pattern which falls off from the centre of the neutron vortex as $\sim 1/r$. The value of B_2 turns out to be $\sim 10^{14}$ G and the resulting vortex number density $n_1 \sim 10^{20}$. The net proton vortex number per neutron vortex is $\sim 10^{13}$ (Sedrakian et al 1983; Paper I).